neurology international

MDPI

Article

Tactile Feedback Device Effects on Sensory-Motor Integration in Post-Stroke Finger Impairment: A Single-Case Experimental Multiple-Baseline Study

Ken Kitai [1,2,*], Kaichi Nishigaya [1,3], Yasuhisa Mizomoto [1], Hiroki Ito [1], Ryosuke Yamauchi [1], Osamu Katayama [1,4], Shin Murata [1] and Takayuki Kodama [1]

[1] Graduate School of Health Sciences, Kyoto Tachibana University, Kyoto 607-8175, Kyoto, Japan; k.nishigaya0913@gmail.com (K.N.); n.y.m0809@gmail.com (Y.M.); h901524007@st.tachibana-u.ac.jp (H.I.); yamauchi-r@tachibana-u.ac.jp (R.Y.); katayama.o@ncgg.go.jp (O.K.); murata-s@tachibana-u.ac.jp (S.M.); kodama-t@tachibana-u.ac.jp (T.K.)
[2] Rehabilitation Department, Maizuru Red Cross Hospital, Maizuru 624-0906, Kyoto, Japan
[3] Rehabilitation Department, Zenjokai Rehabilitation Hospital, Nagoya 457-0046, Aichi, Japan
[4] Department of Preventive Gerontology, National Center for Geriatrics and Gerontology and Social Science Research Center, Obu City 474-8511, Aichi, Japan
* Correspondence: fbgk0311@yahoo.co.jp; Tel.: +81-75-571-1111

Abstract

Background/Objectives: Post-stroke impairment (PSI) frequently causes upper limb sensorimotor deficits, including reduced ability to perceive fingertip friction, limiting dexterous movements. We evaluated the effects of a tactile sensory substitution device ("Yubi-Reco") that delivers real-time fingertip friction information to both temporal bones via vibration and explored potential neurophysiological changes in PSI. Methods: This study used a single-case experimental multiple-baseline design. Three participants with PSI completed a 15-day AB-phase protocol. Baseline (A) consisted of daily sensorimotor tasks without Yubi-Reco, while the intervention (B) added real-time friction feedback via Yubi-Reco to the same tasks. Outcomes included electroencephalography (gamma power), the Purdue Pegboard Test, finger numbness Numerical Rating Scale (NRS), Motor Activity Log-14 (Amount of Use [AoU], Quality of Movement [QoM]), and sense of agency (SoA). Effect sizes were calculated using Tau-U. Results: Very large changes were observed in Purdue Pegboard Test performance (Tau-U = 0.80), and large changes were observed in finger numbness NRS scores (Tau-U = 0.79). Case I showed increased gamma power across frontal and central sites, Case II demonstrated relative attenuation near right frontal and parietal sites, and Case III showed bilateral central gamma reduction, suggesting neurophysiological alterations near recorded sites. AoU and SoA improved in all participants. AoU exceeded the minimal clinically important difference (0.5 points) in two cases. Conclusions: Real-time sensory substitution feedback using Yubi-Reco may improve upper-limb sensorimotor function and induce preliminary neurophysiological changes in individuals with PSI. The intervention appeared to enhance dexterous movement ability and SoA, which coincided with preliminary, exploratory neurophysiological shifts across sensorimotor networks.

Keywords: stroke; sensory substitution; single-case experimental design; Tau-U; electroencephalography; rehabilitation

Check for updates

Academic Editor: David Della-Morte

Received: 13 September 2026
Revised: 16 October 2026
Accepted: 28 October 2026
Published: 2 November 2026

Copyright: © 2026 by the authors. Licensee MDPI, Basel, Switzerland. This article is an open access article distributed under the terms and conditions of the Creative Commons Attribution (CC BY) license.

1. Introduction

A serious and frequent sequela of stroke is sensory and motor dysfunction of the upper limbs and finger sensorimotor impairment [1,2] (referred to in this study as post-stroke impairment, PSI [3]). PSI has a significant impact on daily living ability and quality of life [4]. Sensory feedback is essential to promote functional recovery after PSI [5]. In particular, repeated activation of sensory feedback during purposeful movements may increase motor cortical excitability and improve motor training performance [6]. Such instances occur when motor intention and sensory feedback appropriate for the desired movement are processed synchronously in the brain. Given that feedback delays exceeding 200 ms begin to attenuate the sense of agency (SoA) and delays around 400–500 ms reduce it by approximately half, this tight temporal synchrony is hypothesized to support the emergence of SoA [7]. Rather than a simple deterministic sequence, we propose a theoretical model in which an enhanced SoA may interact with sensorimotor cortical processing, potentially modulating excitability within the premotor cortex and corticospinal pathways to facilitate motor re-learning [8]. Real-time application of visual and electrical stimulation synchronized with hand movements can reportedly enhance gross motor function of the hand [9,10]. Real-time feedback approaches utilizing compensatory sensory modalities report that real-time feedback stimulation enhances the sensorimotor areas in the brain, which are considered important for motor learning, and improves the voluntary control of the fingers. Conversely, although the temporal alignment of motor intention and sensory feedback correlates with the generation of an SoA ($r = 0.28$), studies have reported that this correlation is weak [11]. Manipulation of an object is made possible by the continuous input of friction information generated between the finger pads and the object and the muscle activity of the hand that is in sync with this friction information [12]. Therefore, not only must the motor intention and sensory feedback be synchronized in time, but also feedback must be received on the strength of the friction information continuously obtained from the finger pad. This implies that qualitative elements of sensory feedback are also important. Providing continuous feedback stimuli that correspond to the motor friction generated between the finger pad and the object is difficult. In a review that evaluated sensory feedback interventions for PSI, the effect of rehabilitation using sensory feedback accompanying motor intention was found to be limited [4].

Previously, we demonstrated the proof-of-concept of real-time tactile sensory substitution in post-stroke impairment (PSI) through a single-case study and conceptualized its clinical potential [13]. However, that initial work lacked rigorous verification of internal validity and did not incorporate quantitative neurophysiological evaluations. Although our subsequent study implemented a multiple-baseline design (MBD) [14], it targeted cervical spinal cord injury—a deficit at the sensory relay level—leaving the efficacy of this approach in stroke, where sensory integration itself is impaired, unverified under MBD control. Furthermore, that SCI study restricted its electroencephalographic (EEG) analysis to midline channels, whereas post-stroke brain pathology involves hemispheric lesions and potential interhemispheric compensation, necessitating detailed hemispheric laterality assessments. To address these critical gaps, the present study aimed to expand upon our prior work by applying a staggered MBD across three stroke participants to establish internal validity, while simultaneously conducting quantitative EEG analysis across both midline and bilateral electrode channels. Specifically, we evaluated the treatment effects of real-time friction feedback (Yubi-Reco) on manual dexterity, sensory symptoms, daily hand use, and sense of agency (SoA), while longitudinally tracking neural dynamics. We hypothesized that: (1) introduction of Phase B would induce phase-contingent functional gains and sensory relief beyond baseline trends; (2) real-time feedback would enhance real-world hand activity (MAL-14) and SoA; and (3) longitudinal EEG analysis would

reveal severity- and region-dependent gamma-band modulations, capturing both midline and lateralized interhemispheric neurophysiological shifts.

2. Materials and Methods

2.1. Study Design and Reporting

Participants were in the subacute to early chronic stage of recovery, with post-onset intervals of approximately 69, 86, and 142 days. The overall participant selection process is depicted in the flowchart in Figure 1, their demographic and clinical characteristics are summarized in Table 1, and the study protocol is illustrated in Figure 2. Candidates were identified from inpatients and outpatients in the rehabilitation department based on the predefined inclusion and exclusion criteria. A convenience sampling method was used rather than consecutive sampling. All three eligible patients who were approached gave written informed consent to participate, and no candidates formally declined participation or were excluded prior to entry. Clinical characteristics—including handedness, dominant hand, affected side, concurrent rehabilitation, relevant medications, and neurological comorbidities—were systematically extracted from medical records. The absence of higher brain dysfunction (e.g., aphasia, unilateral spatial neglect, apraxia, or severe attention deficits) was confirmed through comprehensive clinical evaluation by attending physicians, as well as standardized cognitive screening using the Mini-Mental State Examination (MMSE $\geq$ 27) [15] and Trail Making Test Part A (TMT-A < 60 s) [16]. The TMT-A cutoff of 60 s was established based on normative data [16] showing that average completion times remain well under 60 s across healthy adult age groups, thereby ensuring that all participants possessed sufficient visual attention, processing speed, and cognitive capacity to comprehend and comply with the experimental tasks. Specifically, a multiple-baseline design across participants was employed, with staggered baseline durations of 4, 5, and 8 days for Cases I, II, and III, respectively, and interventions beginning on days 5, 6, and 9. Regarding motor eligibility, all participants demonstrated a Brunnstrom Recovery Stage [17] of II or above for the paretic fingers. The severity of finger numbness was evaluated using an 11-point Numerical Rating Scale (NRS), ranging from 0 (no numbness) to 10 (worst imaginable numbness), serving as a subjective symptom rating without categorical severity classification. Finger numbness NRS was evaluated exclusively as a subjective symptom outcome. For the Pain Catastrophizing Scale, a score of 30 was used as the cutoff for clinically significant catastrophic thinking [18]. Motor impairment was assessed using the Fugl-Meyer Assessment for Upper Extremity [19], with scores categorized as severe ($\leq$19), moderate (20–47), and mild ($\geq$48) [20].

Table 1. Basic patient characteristics, Cases I–III.

Characteristic/Assessment	I	II	III
Sex, Age (year)	Male, 81	Female, 60	Male, 64
Height (cm), weight (kg), body mass index	158.0, 56.6, 22.7	161.0, 51.2, 19.8	154.0, 69.0, 29.1
Handedness (Dominant hand)	Right	Right	Right
Affected side	Left	Left	Right
Diagnosis	Right Pontine Infarction	Right Subcortical Hemorrhage	Left Atherothrombotic Cerebral Infarction
Study start date (X = date of stroke onset)	X + about 86 days	X + about 142 days	X + about 69 days
Cognitive Screening & Executive Function			

Table 1. *Cont.*

Characteristic/Assessment	I	II	III
Mini-Mental State Examination score	30/30	30/30	29/30
Trail Making Test Part A completion time (seconds)	47	53	46
Sensory Evaluation			
Numbness Numerical Rating Scale	Left fingers 6	Left fingers 3	Right fingers 6
Superficial sensation	5/10	10/10	10/10
Deep sensation/Kinesthesis	5/5	4/5	5/5
Pain Catastrophizing Scale	Total: 41/52 Rumination: 20/20, Helplessness: 11/20, Magnification: 10/12	Total: 16/52 Rumination: 7/20, Helplessness: 6/20, Magnification: 3/12	Total: 12/52 Rumination: 5/20, Helplessness: 4/20, Magnification: 3/12
Motor & Sensorimotor Function			
Purdue Pegboard Test (Quantity)	0.0	5.0	6.5
Fugl-Meyer Assessment for Upper Extremity	Total: 26/66 Arm: 20/36 Wrist: 0/10 Hand: 6/14 Coordination: 0/6	Total: 48/66 Arm: 25/36 Wrist: 9/10 Hand: 14/14 Coordination: 0/6	Total: 57/66 Arm: 28/36 Wrist: 9/10 Hand: 14/14 Coordination: 6/6
History	Hypertension, diabetes, atrial fibrillation, cerebral infarction	None	Hypertension, diabetes

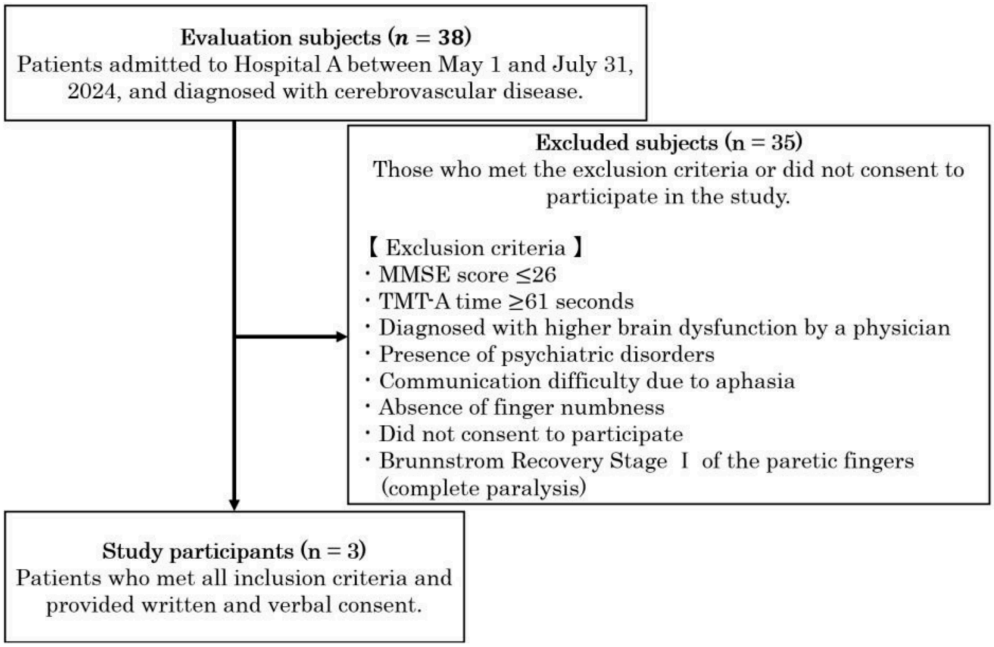


Figure 1. Participant selection flowchart. Flow diagram illustrating the screening, exclusion, and enrollment process for study participants. A total of 38 stroke patients admitted to Hospital A between 1 May and 31 July 2024, were screened for eligibility. Thirty-five candidates were excluded based on predefined exclusion criteria or lack of consent. Ultimately, three patients met all inclusion criteria and were enrolled in the study (Cases I, II, and III). Abbreviations: MMSE, Mini-Mental State Examination; TMT-A, Trail Making Test Part A.

Day	1	2	3	4	5	6	7	8	9	10	11	12	13	14	15
I	A	A	A	A	B	B	B	B	B	B	B	B	B	B	B
II	A	A	A	A	A	B	B	B	B	B	B	B	B	B	B
III	A	A	A	A	A	A	A	A	B	B	B	B	B	B	B

Figure 2. Protocols for multiple-baseline designs across participants. Staggered baseline durations of 4, 5, and 8 days were implemented for Cases I, II, and III, respectively, with interventions A and B beginning on days 5, 6, and 9 according to the steps in the diagram. Gray shading indicates the baseline (Phase A) periods.

The study protocol was approved by the ethics committee of the university (approval number: 23-27).

2.2. Intervention Methods

The method previously described was used as a reference [14].

In dexterous movements, friction information generated when finger pads come into contact with an object is perceived in the brain, and the corresponding muscle activity in the fingers is induced [12,21,22]. To reproduce such unique finger functions, introducing a sensor capable of detecting this friction information with high accuracy is essential. In this study, we used a Finger Recorder (hereafter referred to as Yubi-Reco) (Tech Gihan Co., Ltd., Uji, Japan), a tactile feedback device that detects friction information and presents it as a compensatory vibration stimulus to other body parts in real time. Yubi-Reco detects the friction information generated within the skin when the finger pad comes into contact and measures it as vibration information. A vibration-detection sensor was attached by wrapping it around the distal interphalangeal (DIP) joint of the index finger, and the obtained signal was modulated to a frequency band that humans can perceive. Specifically, the Yubi-Reco device samples contact friction at 1000 Hz and modulates it into vibratory stimuli (50–250 Hz) via bilateral temporal actuators, maintaining a system latency of <15 ms. The modulated vibration information is presented via vibrators attached to both temporal bones. The trigeminal ganglion is within the temporal bone, and the trigeminal nerve is responsible for detecting facial sensations, including vibration, and projecting them to the central nervous system. Therefore, we adopted this compensatory pathway [23]. Treatment fidelity was ensured via standardized therapist supervision, strictly maintaining task parameters and device application across all sessions. Furthermore, the intervention was structured so that real-time, friction-contingent sensory feedback provided an incremental sensory contribution over standard motor practice alone, specifically targeting the integration of tactile information during fine finger movements. To explicitly distinguish sensory outcomes from intervention tasks, finger numbness NRS served as a subjective symptom outcome, whereas the intervention incorporating sandpaper tasks involved active tactile discrimination across five distinct grit sizes.

This study used a Multiple-Baseline Design (MBD) across participants, a single-case experimental design in which the start time of intervention Phase B was intentionally staggered across cases [24]. MBD has been established as a robust methodology for evaluating the effectiveness of sensory-targeted rehabilitation approaches while controlling for confounding factors [25]. Staggered baseline durations of 4, 5, and 8 days were predetermined for Cases I, II, and III, respectively, allowing Phase B interventions to begin on Days 5, 6, and 9. These specific baseline lengths were operationalized based on a combination of clinical-ethical considerations and observational requirements. In a clinical rehabilitation environment for subacute stroke patients, extending unintervention baseline phases unnecessarily presents ethical concerns regarding delayed targeted therapy. Thus, baseline periods were designed to collect the minimum required data points to establish behavioral stability and confirm the absence of pre-intervention therapeutic trends prior to Phase B. Furthermore, the contrasting ratio of Phase A and Phase B durations across participants—

ranging from a shorter baseline with a longer intervention phase in Case I (Phase A: 4 days vs. Phase B: 11 days) to a longer baseline in Case III (Phase A: 8 days vs. Phase B: 7 days)—was an intentional structural feature of our staggered design. A longer baseline in Case III allowed for extended monitoring to rule out spontaneous recovery or practice trends prior to treatment, whereas a longer Phase B in Case I ensured sufficient intervention exposure to evaluate cumulative sensorimotor adaptation in a more severely impaired participant. Crucially, this reciprocal variation in phase durations naturally arises from staggering the initiation of treatment within a fixed total study duration, demonstrating that performance shifts occur contingently upon the introduction of Phase B regardless of baseline length. To eliminate the influence of baseline trends and evaluate the pure effect of Phase B, trend corrections were incorporated into the Tau-U analysis [26]. Across the 15-day protocol, Phase A (baseline) comprised 4–8 daily sessions during which participants performed the standardized 30 min sensorimotor task protocol without the Yubi-Reco device. In Phase B (intervention, 7–11 daily sessions), participants performed the exact same task protocol while wearing the Yubi-Reco device to receive real-time friction feedback. Thus, task parameters, duration, and supervisory conditions were held constant across both phases, with the presence of real-time friction feedback being the sole manipulated independent variable (Figure 2). The actual number of measurement points per phase was systematically determined according to the staggered multiple-baseline design. Specifically, the baseline phase (Phase A) comprised 4 data points for Case I, 5 data points for Case II, and 8 data points for Case III. The intervention phase (Phase B) comprised 11 data points for Case I, 10 data points for Case II, and 7 data points for Case III. All completed measurements were retained in the primary outcome analyses, and no behavioral, NRS, or physiological data were excluded.

The daily intervention consisted of three sensorimotor tasks performed for 10 min each (totaling 30 min per session) under strict one-on-one therapist supervision. Box and Block Test and Peg task performance were considered to reflect manual dexterity [27,28]. Each session followed a standardized sequence: (1) block stacking using square wooden blocks from the Box and Block Test (10 min, focusing on grasp-and-release repetitions), (2) peg manipulation (10 min, aiming for maximum precise peg insertions), and (3) tactile discrimination training for 10 min, in which participants actively discriminated surface textures applied to the ventral index finger pad [4]. Five grit sizes (#40, #80, #150, #240, and #400) were presented in a randomized order, and participants were instructed to touch each surface and discriminate differences in roughness. Therapists provided standardized verbal instructions asking participants to perform each task as accurately as possible while focusing on tactile sensations from their fingers. From Phase B onward, the subjects were required to wear a Yubi-Reco while performing each motor task.

Longitudinal pre- and post-assessments were also performed. Longitudinal assessment included daily neurophysiological, motor, and sensory function assessments. The pre- and post-intervention assessments included motor activity and real-world functional transfer assessments before phase A began, after phase A ended (before intervention B), and after phase B ended.

For the longitudinal neurophysiological assessment, electroencephalography (EEG) activity was recorded for 1 min immediately following each motor task session, performed twice daily (yielding a total of two 1 min EEG recordings per day) during the Peg task, maintaining a standardized acquisition schedule. EEG measurements were performed in a quiet environment with the participants seated in a relaxed state without using the Yubi-Reco device. Because EEG recordings were conducted off-line (without device attachment), the observed modulations reflect sustained, cross-phase shifts in neurophysiological activity (cumulative adaptation across baseline and intervention phases) rather than immediate,

online stimulus-evoked effects during active feedback. EEG was recorded using a portable electroencephalograph (StEEG) (Creact Co., Ltd., Tokyo, Japan). Electrode placement conformed to the international 10–20 system, with both earlobes used as reference electrodes at eight locations: Fp1, Fp2, C3, C4, O1, O2, Fz, and Pz. The sampling frequency was set to 1000 Hz. Sensory function was assessed using the NRS as a subjective index of finger numbness. The evaluations were conducted once daily after the motor task. We used the Motor Activity Log-14 (MAL-14) to assess learning changes and changes in upper limb use [29]. Participants were assessed on 14 daily activities using two indices: Amount of Use (AoU) and Quality of Movement (QoM), both rated on a 6-point scale (0–5). Additionally, to evaluate the relationship between behavioral changes and the sense of agency (SoA), participants rated each MAL-14 item using a SoA NRS (0 = not at all, 10 = extremely strong feeling of performing the movement oneself) [14]. This multifaceted assessment aimed to capture changes not only in patients' functional motor performance but also in their active motor awareness and sensorimotor cognitive processing. Safety and feasibility were systematically monitored at every session by tracking potential adverse events, including local discomfort, skin irritation at vibrator attachment sites, headache, dizziness, fatigue, or stimulation intolerance.

2.3. Analysis Method

Independent component analysis (ICA) was applied as a preprocessing step to decompose the mixed EEG signals into statistically independent sources. ICA models multidimensional EEG recordings as linear combinations of statistically independent non-Gaussian components [30]. We performed ICA using the EEGLAB toolbox in MATLAB R2023b [31], employing the FastICA algorithm. To minimize potential electromyographic (EMG) artifact contamination in the high-frequency gamma band (40–100 Hz), participants were explicitly instructed to relax their jaw and facial muscles during recordings. Prior to time–frequency analysis, raw EEG traces were visually inspected to systematically reject epochs contaminated by transient high-amplitude muscle bursts, sharp electromyographic spikes, or ocular artifacts. While ICA was employed for primary source separation and ocular artifact rejection, muscle electrical activity is spatially distributed and spectrally overlaps with neural gamma oscillations; therefore, strict visual epoch rejection and relaxation instructions were prioritized to mitigate EMG contamination rather than relying solely on IC component removal, particularly for anterior channels (FP1 and FP2). Furthermore, electrophysiological analyses paid specific attention to central channels (C3 and C4) over the primary motor cortex, which are anatomically less susceptible to temporal or cervical muscle attachment interference. Time–frequency decomposition of the ICA-cleaned EEG data was performed using continuous Morlet wavelet transforms in MATLAB R2023b. For each electrode, power spectral density was computed in microvolts squared per Hertz ($\mu V^2/Hz$) and transformed using log10(power + 1) to yield log-transformed gamma-band power values ($\log10[\mu V^2/Hz + 1]$), which served as the primary computational units for subsequent analyses [32]. Gamma-band power (40–100 Hz) was extracted to assess neural activity, and for each time segment and electrode, gamma-band power across frequency bins was summarized using the geometric mean to obtain a single representative value. For each assessment day, the metrics from the two daily 1 min EEG recordings were averaged to yield a single daily neurophysiological value per electrode. The electrodes analyzed for hemispheric laterality were FP1 and FP2 (frontal) and C3 and C4 (central), and midline activity was assessed using Fz (frontal) and Pz (parietal). The gamma-band power values exported from MATLAB were imported into Excel, where condition-wise means and standard errors of the mean were calculated for each electrode and task phase.

The values obtained in each phase of the Peg Test, numbness NRS, and EEG were subjected to Tau-U calculations to determine the effect size, a statistical indicator of the magnitude of the effect. Derived from Kendall's rank correlation and the Mann–Whitney U test, Tau-U is a non-parametric metric that quantifies phase non-overlap while controlling for monotonic trends without requiring parametric distributional assumptions [33]. For each phase contrast, all pairwise comparisons between data points were evaluated chronologically and scored as positive (+: improvement), negative (−: deterioration), or tied (T). The score statistic S was calculated as S = pos − neg, and the non-overlap effect size was determined as:

$$\text{Tau-U} = S/\text{pairs}$$

where pairs = nA × nB for between-phase contrasts (nA and nB represent the number of data points in Phase A and Phase B, respectively). For outcomes where lower values indicate clinical improvement (such as numbness NRS), scores were reverse-coded so that positive Tau-U values consistently reflect beneficial intervention effects. Prior to evaluating overall intervention effects, Phase A was evaluated for monotonic trends; when a statistically significant baseline trend was identified, baseline trend control (A vs. B—Trend A) was applied by subtracting internal Phase A trend score pairs (SA) from the overall S statistic [pairs = (nA × nB) + nA(nA − 1)/2]. Furthermore, the omnibus combined Tau-U across the three cases was calculated by weighting each case according to its number of paired comparisons, dividing the sum of S statistics across cases by the sum of total pairs (S_total/pairs_total) [33]. Statistical significance was evaluated using standard error SES to derive Z-scores (z = S/SES) and exact permutation *p*-values.

The effect of intervention B was verified by considering the influence of natural recovery and phase A. The effect assessment by Tau-U was classified as "no change or small change" when the value was 0 to 0.19, "moderate change" when it was 0.20 to 0.59, "large change" when it was 0.60 to 0.79, and "very large change" when it was 0.80 to 1.00 (values of exactly 0.80 were classified as "very large change") [34]. Stable baselines with zero variance (e.g., Case I NRS 6.00 +/− 0.00; Case II NRS 3.00 +/− 0.00) reflect perfect baseline stability, resulting in a baseline trend S statistic of zero and allowing pure A vs. B pairwise evaluation without baseline noise or ties. Given the exploratory single-case design evaluating 6 electrode channels across 3 cases, unadjusted *p*-values are reported, and channel-wise electrophysiological comparisons should be interpreted as exploratory hypothesis-generating metrics. The Tau-U analysis was conducted using the web application Single Case Study Web-Based Calculator for SCR Analysis (version 2.0) [35], with the baseline correction option enabled. For visual evaluation, electrode-level gamma-band power changes (Tau-U effect sizes) were mapped using BrainNet Viewer [36]. Node information was encoded in MATLAB and projected onto a template three-dimensional brain surface, with node colors assigned based on Tau-U values. Note that nodes represent scalp recording electrode locations rather than cortical source localizations or functional connectomic networks. For the pre- and post-assessments, each item on the MAL-14 AoU and QoM was rated on a 6-point scale from 0 to 5, with the total score divided by the number of items to obtain the final score. For the SoA NRS, each item was rated on a 0–10 scale, with the total score divided by the number of items to obtain the final score. These scores were compared between the phases to verify the effects of the intervention from multiple perspectives.

Device Status Statement: The device used in this study (Finger Recorder) is a commercially available device and is not approved as a medical device by any regulatory authority.

2.4. Use of GenAI

During the preparation of this work the authors used Gemini (Google LLC, Mountain View, CA, USA) to translate text, reduce the word count, and improve the readability. After using this tool/service, the authors reviewed and edited the content as needed and take full responsibility for the content of the publication.

2.5. Evaluator Blinding and Treatment Fidelity

Due to the single-arm, proof-of-concept nature of this single-case experimental study, outcome assessments were conducted by non-blinded physical therapists. To maximize treatment fidelity, all intervention sessions were delivered strictly on a one-on-one basis following a standardized operational checklist (including fixed task durations, sequential order, and standardized verbal instructions). Protocol adherence was monitored across all sessions, with 100% completion of the planned training components.

3. Results

All three participants completed the full intervention protocol without any session interruptions. No adverse events—including local discomfort, skin irritation, headache, dizziness, fatigue, or stimulation intolerance—were reported throughout the study, confirming the safety and feasibility of the protocol.

Table 2 and Figures 3 and 4 detail EEG gamma power changes and Tau-U effect sizes. Case I showed increased gamma power, notably near the left frontal site (Fp1, Tau-U = 0.80) and midline frontal site (Fz, Tau-U = 0.53). Case II exhibited a moderate negative change near the right frontal site (Fp2, Tau-U = −0.30). Case III showed a large negative change near the right central site (C4, Tau-U = −0.68) (Table 2, Figures 3 and 4).

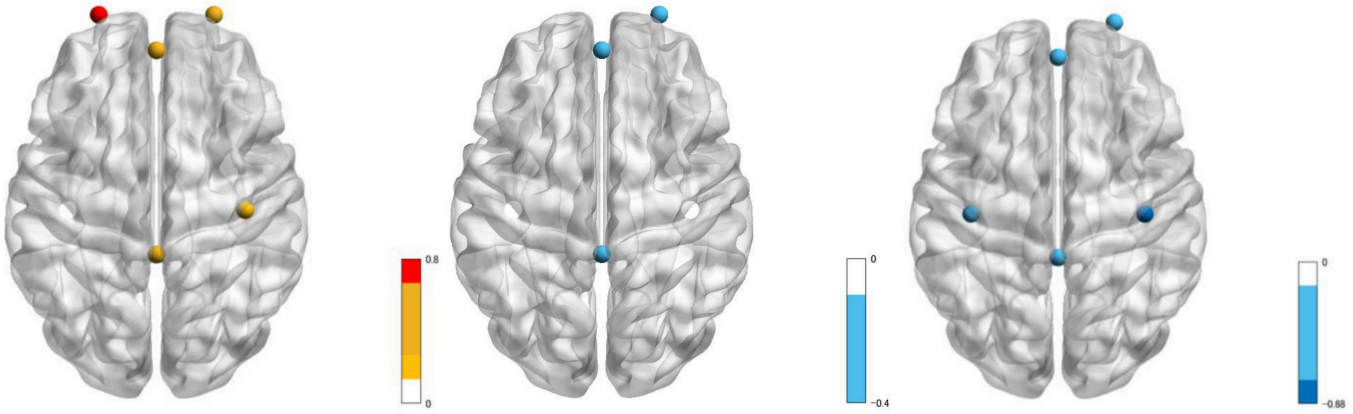


Figure 3. 3D surface visualization of electrode-level gamma-band power changes (Tau-U effect sizes). Nodes represent scalp recording electrode positions (Fp1, Fp2, C3, C4, O1, O2, Fz, and Pz) mapped onto a template brain surface, rather than cortical source localizations or functional connectomic networks. Node color indicates the magnitude and direction of intervention-induced gamma-band power shifts evaluated via Tau-U (red/warm colors represent positive shifts/increased power; blue/cool colors represent negative shifts/decreased power). From left to right: Case I, Case II, and Case III.

Table 2. EEG results, Cases I–III.

	Fp1 (dB)			Fp2 (dB)			C3 (dB)			C4 (dB)			Fz (dB)			Pz (dB)		
	A AVG ± SE	B AVG ± SE	Tau-U	A AVG ± SE	B AVG ± SE	Tau-U	A AVG ± SE	B AVG ± SE	Tau-U	A AVG ± SE	B AVG ± SE	Tau-U	A AVG ± SE	B AVG ± SE	Tau-U	A AVG ± SE	B AVG ± SE	Tau-U
I	2.03 ± 0.03	2.27 ± 0.07	0.80	2.29 ± 0.06	2.43 ± 0.07	0.39	2.11 ± 0.08	2.25 ± 0.10	0.07	2.39 ± 0.06	2.47 ± 0.03	0.25	2.06 ± 0.07	2.25 ± 0.08	0.53	2.14 ± 0.10	2.26 ± 0.06	0.27
II	2.04 ± 0.08	2.02 ± 0.07	−0.08	2.07 ± 0.04	2.01 ± 0.19	−0.30	2.36 ± 0.05	2.40 ± 0.06	0.08	2.59 ± 0.12	2.59 ± 0.06	−0.04	2.73 ± 0.20	2.58 ± 0.14	−0.40	3.11 ± 0.11	2.97 ± 0.16	−0.32
III	2.52 ± 0.16	2.48 ± 0.08	−0.18	2.60 ± 0.14	2.42 ± 0.07	−0.32	2.99 ± 0.09	2.80 ± 0.20	−0.38	2.72 ± 0.10	2.39 ± 0.08	−0.68	3.19 ± 0.16	2.81 ± 0.19	−0.27	2.77 ± 0.13	2.58 ± 0.08	−0.25

The changes in neural activity patterns observed after intervention varied between the cases, suggesting that potential neurophysiological shifts coincided with the severity of functional impairment in each case. EEG, electroencephalography; dB: decibel, AVG: average, SE: standard error.

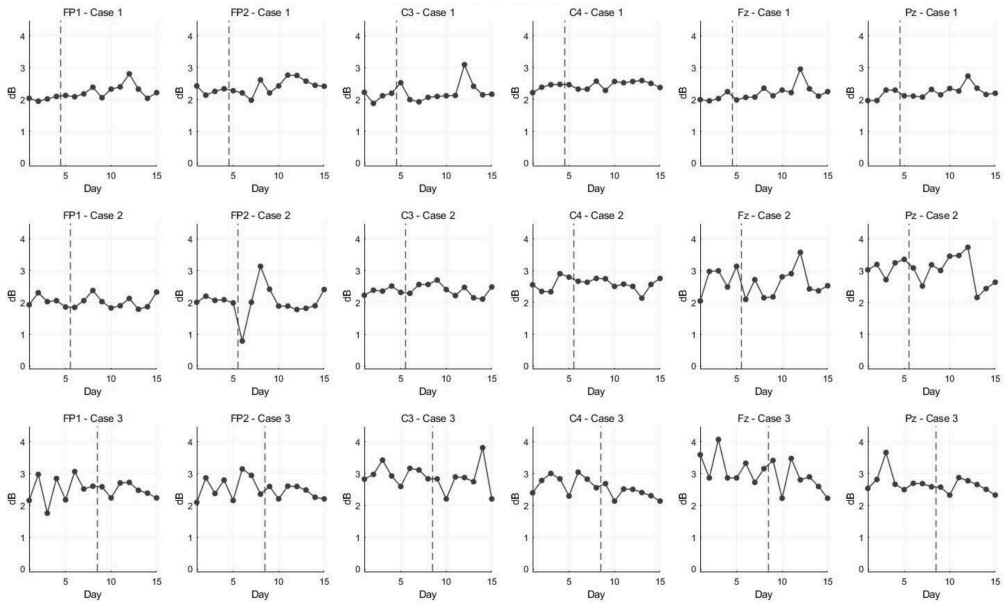


Figure 4. Daily longitudinal trajectories of EEG gamma-band power across electrode channels for Cases I–III. Individual daily log-transformed gamma-band power values (dB) recorded at six scalp electrodes (Fp1, Fp2, C3, C4, Fz, and Pz) across the 15-day protocol for Case I (**top row**), Case II (**middle row**), and Case III (**bottom row**). Vertical dashed lines mark the phase transition from baseline (Phase A) to intervention with Yubi-Reco (Phase B) on Day 5 for Case I, Day 6 for Case II, and Day 9 for Case III. Note that EEG recordings were acquired off-line immediately following daily motor training sessions, capturing sustained, cross-phase neurophysiological shifts.

The Purdue Pegboard Test showed overall improvements across cases (combined Tau-U = 0.80). Individually, statistically significant improvements were observed in Case II (p = 0.0101) and Case III (p = 0.0065), whereas Case I demonstrated descriptive improvement that did not reach statistical significance (p = 0.1172, 90% CI [-0.027, 1.000]). (Table 3, Figure 5). However, individual responses varied across cases. Specifically, statistically significant improvements were observed in Case II (Tau-U = 0.86, p = 0.0101) and Case III (Tau-U = 0.86, p = 0.0065), whereas Case I showed a descriptive improvement that did not reach statistical significance (Tau-U = 0.62, p = 0.1172, 90% CI [−0.027, 1]). Similarly, for the finger numbness NRS, the combined Tau-U indicated a large overall effect size (combined Tau-U = 0.79) (Table 4, Figure 6). Statistically significant changes were revealed in Case I (Tau-U = 0.95, p = 0.0090) and Case III (Tau-U = 0.70, p = 0.0279). Meanwhile, Case II showed a large effect size (Tau-U = 0.75), representing a strong statistical trend rather than conventional significance (p = 0.0662). Furthermore, daily functioning and subjectively perceived agency as measured by the Motor Activity Log-14 (AoU and QoM) and SoA NRS showed consistent positive shifts following intervention Phase B across all participants (Table 5).

Table 3. Purdue Pegboard Test results, Cases I–III.

	A AVG ± SE	B AVG ± SE	Tau-U	SD	Z	*p* Value	CI 90%
I	0.13 ± 0.13	1.05 ± 0.96	0.62	15.32	1.57	0.1172	−0.027<>1
II	5.20 ± 0.12	6.35 ± 0.15	0.86	16.33	2.57	0.0101	0.303<>1
III	6.75 ± 1.04	9.67 ± 0.84	0.86	17.28	2.72	0.0065	0.332<>1
Combined			0.80				

<>: indicates the 90% confidence interval.

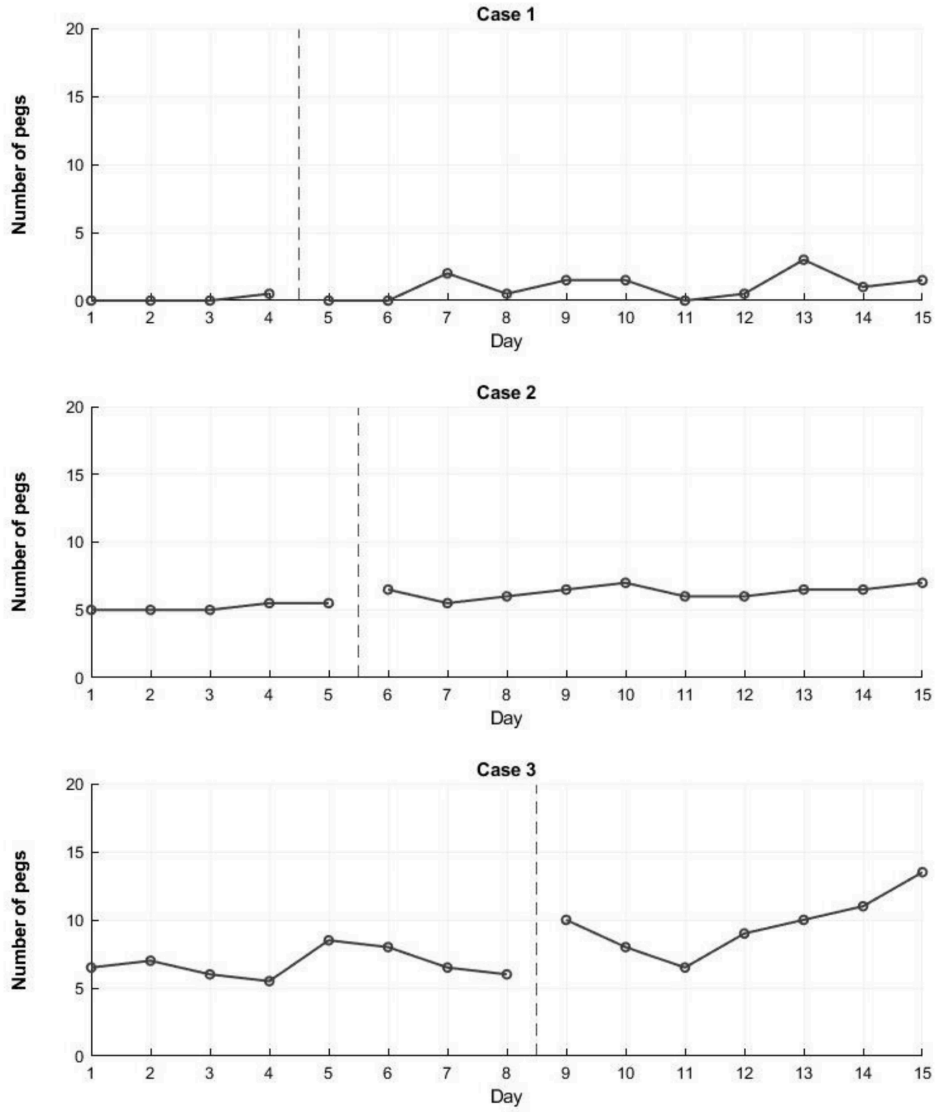


Figure 5. Daily longitudinal trajectories of Purdue Pegboard Test performance for Cases I–III. Individual daily peg insertion counts across the 15-day protocol for Case 1 (**top**), Case 2 (**middle**), and Case 3 (**bottom**). Vertical dashed lines indicate the onset of Phase B (Yubi-Reco intervention) on Day 5 for Case 1, Day 6 for Case 2, and Day 9 for Case 3. Visual analysis illustrates immediate level shifts and progressive upward trends following intervention onset in Cases 2 and 3, whereas Case 1 demonstrated modest descriptive gains constrained by severe baseline motor deficits.

Table 4. Numbness NRS results, Cases I–III.

	A AVG ± SE	B AVG ± SE	Tau-U	SD	Z	*p* Value	CI 90%
I	6.00 ± 0.00	4.55 ± 0.69	0.95	15.32	2.61	0.0090	0.336<>1
II	3.00 ± 0.00	2.10 ± 0.28	0.75	16.33	1.84	0.0662	0.063<>1
III	5.63 ± 0.52	2.33 ± 0.47	0.70	17.28	2.20	0.0279	0.171<>1
Combined			0.79				

Tau-U analysis revealed a large change in two of three cases and a very large change in one of three cases. A large change was observed in combined analyses. Note: Combined Tau-U indicated a large overall effect. Statistically significant changes were observed in Cases I and III, whereas Case II reflected a strong statistical trend (p = 0.0662). AVG: average, SE: standard error, SD: standard deviation, CI 90%: 90% confidence interval, <>: indicates the 90% confidence interval.

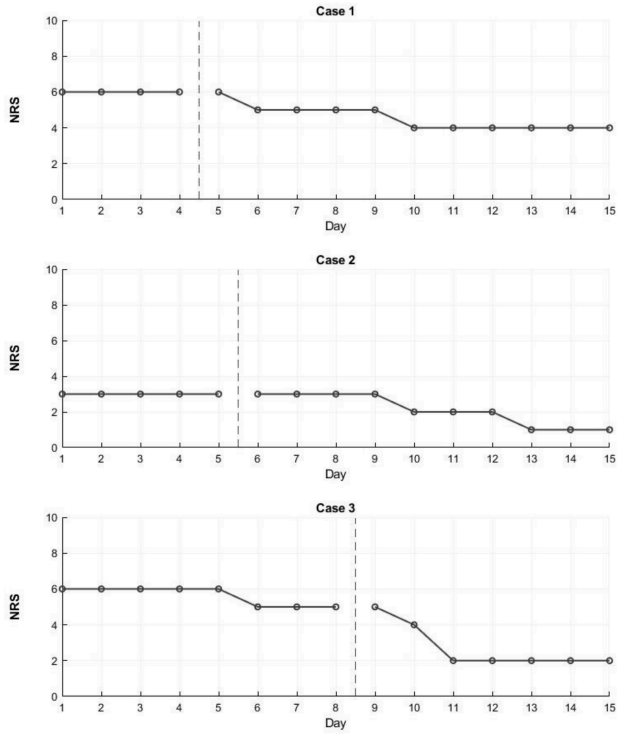


Figure 6. Daily longitudinal trajectories of finger numbness Numerical Rating Scale (NRS) scores for Cases I–III. Individual daily finger numbness NRS ratings across the 15-day protocol for Case 1 (**top**), Case 2 (**middle**), and Case 3 (**bottom**). Vertical dashed lines indicate the phase transition from baseline (Phase A) to Yubi-Reco intervention (Phase B) on Day 5 for Case 1, Day 6 for Case 2, and Day 9 for Case 3. Visual analysis illustrates consistent step-down reductions in subjective numbness ratings following intervention onset across all cases, reflecting meaningful sensory symptom relief.

Table 5. Motor Activity Log-14 results, Cases I–III.

I	AoU	QoM	SoA
Initial	2.33	2.17	4.17
A	2.67	2.83	4.17
B	3.33	3.33	6.50
II	AoU	QoM	SoA
Initial	3.30	3.55	7.70
A	3.45	3.75	7.70
B	3.70	3.85	8.40
III	AoU	QoM	SoA
Initial	2.88	3.00	4.75
A	3.17	3.17	5.25
B	3.79	3.88	5.83

All patients showed improvement across all items. AoU: amount of use, QoM: quality of movement, SoA: numerical rating scale for sense of agency.

Visual analysis of the daily longitudinal plots (Figures 4–6) demonstrated that functional improvements, sensory symptom relief, and neurophysiological shifts were directly contingent upon the onset of Phase B rather than the passage of time. Specifically, in Case III (8-day baseline), Purdue Pegboard performance (Figure 5) and numbness NRS scores (Figure 6) remained stable throughout the extended baseline phase (Days 1–8) and exhibited immediate level shifts and progressive improvements following Phase B initiation on Day 9. Similarly, Cases I and II demonstrated distinct phase-contingent level shifts coinciding

precisely with Phase B onset on Days 5 and 6, respectively, confirming that the observed changes were driven by the Yubi-Reco intervention rather than time-dependent natural recovery across the 15-day timeline.

Tau-U analysis revealed a large change in one patient and very large changes in two patients. The combined data indicated very large changes. Note: While the combined Tau-U demonstrated a very large effect size, individual analysis showed significant improvements in Cases II and III, whereas Case I exhibited a descriptive improvement that did not reach statistical significance ($p = 0.1172$). AVG: average, SE: standard error, SD: standard deviation, CI 90%: 90% confidence interval, <>: indicates the 90% confidence interval.

4. Discussion

4.1. Case Characteristics and Interpretation

In this study, intervention using Yubi-Reco was performed for three PSI cases. As a result, for the Peg Test, while all cases showed descriptive improvements, statistical significance was reached in Cases II and III, whereas Case I demonstrated a descriptive trend (Tau-U = 0.62, $p = 0.1172$). Similarly, for finger numbness NRS, statistically significant reductions were observed in Cases I (Tau-U = 0.95, $p = 0.0090$) and III (Tau-U = 0.70, $p = 0.0279$), whereas Case II exhibited a large effect size representing a strong statistical trend rather than conventional significance (Tau-U = 0.75, $p = 0.0662$).

In Case I, electroencephalographic gamma power increased near bilateral frontal scalp electrodes (Fp1/Fp2, Tau-U: 0.39–0.80), the right central electrode (C4, Tau-U: 0.25), and midline electrodes (Fz/Pz, Tau-U: 0.27–0.53). The somatosensory area accurately reproduces hand shape in the brain, integrates the necessary motor commands, and selectively activates the muscles required for activities such as manipulating objects [37]. The premotor cortex, supplementary motor area, and prefrontal cortex prepare and execute movements based on sensory information received from the somatosensory area [38–40], as supported by non-human primate models [39]. The probability of bilateral neural recruitment increases with the severity of paralysis, and hand motor function is related to the size of the bilateral sensorimotor cortex [40]. In Phase B, increased neural activity in the sensorimotor area was associated with improvements in finger movements corresponding to dexterous tasks, which may be consistent with the large changes observed in the Peg Test. In laterality assessment during finger movements, neural activity is thought to be strong on the side of the body in the primary motor cortex [41]. The right central electrode site (C4, Tau-U: 0.25) showed greater effects than the opposite side, suggesting that the modulation of electrophysiological activity near the affected sensorimotor recording site could potentially reflect enhanced neural recruitment during motor task performance, while acknowledging that 8-channel EEG has limited spatial resolution. Regarding sensory function, the prefrontal cortex acts on the descending pain inhibitory and pain-modulating systems [42]. Extrapolating from basic neural circuit models [43], relevant sensory input during movement may allow sensorimotor regions to suppress irrelevant sensory noise and reinforce critical feedback. Therefore, coordinated shifts across frontal and central electrode channels may be associated not only with motor function but also with sensory modulation, which could potentially reflect the very large changes observed in the NRS for numbness.

In Case II, the EEG laterality assessment revealed a moderately negative change (Tau-U: −0.30) near the right frontal electrode (Fp2) during Phase B. This suggests that overactivity of gamma waves in the prefrontal cortex may be linked to gating disorders [44]. Case II suggested that reduced gamma power near the right frontal electrode was accompanied by a marked improvement in numbness as measured by the NRS. In midline assessment, a moderate negative change (Tau-U: −0.32) was also observed near the parietal electrode site (Pz). In individuals with well-recovered motor function, neural activation

within sensorimotor areas is reported to be reduced during task performance, reflecting greater computational efficiency [40]. As suggested by basic cellular neurophysiological models [45], efficient sensorimotor processing during movement execution is thought to filter redundant sensory inputs. These changes could potentially reflect more efficient sensorimotor processing near parietal recording channels during dexterous movements, which was associated with suppressed numbness and improved dexterity.

In Case III, a large negative change (Tau-U: −0.68) was observed near the right central electrode site (C4), and a moderate negative change (Tau-U = −0.38) was observed near the left central electrode site (C3). Furthermore, a moderately negative change (Tau-U: −0.27 to −0.25) was observed near midline electrode sites (Fz/Pz). While sensorimotor scalp channels capture key electrophysiological dynamics during finger movements, the observed reduction in gamma power likely reflects enhanced neural efficiency near the recording sites—suppressing redundant electrophysiological recruitment and sensory noise to improve motor performance [41,43]. These findings may be consistent with optimized sensory processing near central recording channels, which could potentially reflect adaptive movement strategies alongside reduced numbness sensations.

Furthermore, because participants entered the study in the subacute to early recovery phase (approximately 69, 86, and 142 days post-stroke) rather than the chronic phase, the potential contribution of spontaneous neurological recovery must be carefully considered alongside intervention effects. While the staggered introduction of the Phase B intervention within our multiple-baseline design helps mitigate time-dependent threats to internal validity, the observed functional and neurophysiological gains may reflect a combination of real-time sensory feedback effects and ongoing natural neural recovery. In summary, the contrasting directional shifts in gamma power—increased power in Case I versus decreased power in Cases II and III—can be conceptualized as a severity-dependent spectrum of neurophysiological adaptation. For severe impairment (Case I), tactile feedback appears to facilitate the recruitment of additional sensorimotor resources near the recorded electrodes. For mild-to-moderate impairment (Cases II and III), the attenuation of gamma power likely reflects the suppression of redundant electrophysiological activity. Rather than proposing definitive neurofunctional mechanisms, concepts such as "bottom-up sensory integration" or "internal model optimization" are utilized here solely as broad, conceptual working hypotheses to help structure these electrode-level observations for future investigation.

4.2. Motor Activity and Real-World Transfer Assessment

Regarding MAL, the AoU of cases I and III was higher in phase B than in phase A. The minimal clinically important difference exceeded 0.5 [46]. Gamma wave modulations in the sensorimotor cortex reflect the state of comparison between motor predictive intention and sensory feedback [47]. Previous literature suggests that real-time sensory feedback congruent with motor intention may facilitate the emergence of SoA, which in turn is thought to support motor re-learning [48]. While established studies indicate that AoU and SoA are correlated [49] and that affected primary motor cortex recruitment helps overcome learned non-use [50], the complex interplay between real-time tactile substitution, agency, and cortical dynamics should be understood as a working hypothesis rather than an established sequential fact. Building on this background, the current intervention resulted in improvements exceeding the MCID of the AoU in both Cases I and III, suggesting that the observed gains may reflect distinct patterns of neural reorganization depending on the severity of paralysis. Specifically, Patient I, who presented with severe paralysis, showed increased gamma power near the affected central electrode site, whereas Patient III, who presented with mild paralysis, exhibited a pattern of decreased gamma power, which could potentially reflect more efficient neural processing near the recording sites.

Importantly, beyond statistical effect-size metrics (Tau-U), these improvements in MAL-14 scores exceeded established Minimal Clinically Important Difference thresholds, confirming that the observed gains represent clinically meaningful functional changes.

The clinically meaningful functional improvements and neurophysiological shifts observed in this study may be closely linked to the unique physiological characteristics of real-time friction substitution. Unlike conventional visual or auditory feedback, which relies on indirect cognitive translation and increases mental workload, or static vibrotactile cues, dynamic object manipulation depends on continuous friction signals at the fingertip to rapidly update internal motor prediction models [12]. Delivering these friction signals via bone-conducted vibration to bilateral temporal regions utilizes the intact cranial trigeminal nerve pathway [23], offering an effective sensory bypass for stroke patients with damaged spinal-thalamic ascending pathways. Furthermore, bilateral temporal stimulation recruits interhemispheric sensorimotor networks, facilitating cortical integration and the emergence of a sense of agency without physically restricting movement of the paretic hand. This aligns with recent concepts in advanced neural interfaces, which emphasize that bidirectional information exchange—coupling motor intention with closed-loop sensory feedback—is essential for achieving intuitive motor control [51]. While invasive neuroprosthetic modalities target amputees [51], our non-invasive tactile substitution framework successfully adapts this closed-loop concept to stroke rehabilitation.

4.3. Limitations

Several methodological and analytical limitations of this preliminary study must be acknowledged. First, the small sample size (N = 3) and clinical heterogeneity regarding lesion sites and baseline severity limit the generalizability of our findings. Second, because participants were in the subacute to early chronic stage (post-onset intervals of ~69–142 days), the potential contribution of spontaneous neurological recovery cannot be fully ruled out. Third, the study employed a single-arm, unblinded design without a sham control condition or blinded evaluators, introducing potential therapist/evaluator bias. Crucially, the intervention inevitably incorporates non-specific therapeutic factors beyond real-time friction feedback, including mechanical vibration, heightened attentional focus toward the paretic hand, device novelty, and generalized sensory stimulation. Because a sham condition utilizing delayed, random, or uncoupled mechanical vibration was not implemented, we cannot definitively determine whether the observed clinical and neurophysiological shifts derived specifically from real-time friction-linked sensory feedback or were partly influenced by these non-specific elements and patient expectations. Additionally, because the Peg Test served as both a daily training task and the primary outcome measure, repeated daily testing inherently introduces potential practice and learning effects. Similarly, daily Numerical Rating Scale (NRS) self-reports may have been influenced by expectancy and placebo effects associated with the use of a novel device.

Furthermore, specific limitations regarding subjective rating scales warrant consideration. The reduction in numbness NRS in mild baseline cases (such as Case II, NRS = 3.0 to 2.1) was constrained by a floor effect, limiting the measurable scope of clinical improvement for sensory symptoms. Future research should establish severity-stratified protocols, prioritizing fine motor dexterity for mild cases while targeting sensory relief in severe cases. In addition, while the Sense of Agency Numerical Rating Scale (SoA-NRS) was used alongside the MAL-14 to capture subjective movement awareness, this scale lacks formal psychometric validation in post-stroke populations. Therefore, changes in both numbness and SoA NRS scores should be interpreted cautiously as exploratory indicators rather than definitive standardized metrics.

Regarding neurophysiological assessments, our EEG setup was limited to an 8-channel montage, which restricts spatial resolution and precludes inverse source localization analysis. Additionally, high-frequency EEG signals—particularly in the gamma band (40–100 Hz)—might remain susceptible to minor residual contamination from craniofacial muscle activity, particularly at anterior channels (Fp1 and Fp2) located near facial/frontalis musculature, despite strict visual epoch rejection. Therefore, the observed gamma-band modulations should be interpreted cautiously as suggestive of potential neurophysiological shifts rather than definitive cortical source-localized neural reorganization. Furthermore, because EEG signals were recorded in an off-line state without the Yubi-Reco device attached, our physiological outcomes specifically capture sustained cross-phase shifts and cumulative neural reorganization across phases, rather than immediate online sensory-evoked feedback modulations.

From an analytical standpoint, evaluating 6 scalp electrode channels across 3 cases without formal alpha adjustment for multiple comparisons increases the risk of Type I error. Unadjusted *p*-values were reported to prevent Type II errors in this preliminary investigation, and electrophysiological findings across multiple channels should be interpreted with appropriate caution. Additionally, the 4-point baseline in Case I represents a potential source of instability when applying Tau-U trend corrections, as statistical power and trend estimation in single-case metrics can be sensitive to short baseline phases.

Finally, the short intervention duration and absence of a long-term follow-up limit our ability to evaluate the retention and long-term sustainability of the observed functional and neurophysiological shifts. Future prospective studies incorporating larger, randomized controlled cohorts with sham conditions and high-density EEG are required to validate these exploratory observations.

5. Conclusions

An intervention using this device was performed in three patients with PSI. The Peg Test showed a very large change in the combined effect size across all three cases, whereas the numbness NRS showed a large change. In the EEG analysis of Case I, with moderate-to-severe PSI, gamma power increased across sensorimotor electrode sites, which may be interpreted within a speculative bottom-up sensory integration framework. In Cases II and III, with moderate-to-mild PSI, gamma power near sensorimotor electrode channels showed relative attenuation, which aligns with a speculative framework of internal model optimization. Overall, rather than establishing direct neurofunctional proof, these exploratory observations offer a highly speculative framework of potential sensorimotor reconstruction according to PSI severity, serving solely as a working hypothesis to guide future research rather than definitive mechanistic conclusions. The results of the sensorimotor function, neurophysiological, and real-world motor activity assessments (MAL-14) showed consistent improvements in sensorimotor function in all three cases across staggered intervention periods, indicating that the staggered experimental structure helped mitigate time-dependent threats to internal validity within single-case constraints. This is consistent with the findings of an intervention study using MBD and Yubi-Reco in individuals with varying degrees of sensorimotor impairment of the fingers following cervical spinal cord injury [14].

Overall, these findings suggest that Yubi-Reco may improve sensorimotor function, though results remain exploratory and warrant further controlled trials. Studies with a greater number of cases and statistical verification are warranted to further verify the effectiveness of this device. Additionally, the absence of a long-term post-intervention follow-up limits our conclusions regarding the durability and retention of these clinical gains. By combining long-term follow-up and neuroimaging analyses,

further elucidating the mechanism of action and verifying the possibility of its clinical application is also necessary.

Author Contributions: Conceptualization, K.K. and T.K.; methodology, K.K. and T.K.; software, K.K. and T.K.; validation, K.K. and T.K.; formal analysis, K.K., K.N. and T.K.; investigation, K.K., K.N. and Y.M.; resources, K.K., H.I. and T.K.; data curation, K.K. and R.Y.; writing—original draft preparation, K.K.; writing—review and editing, K.K., O.K., S.M. and T.K.; visualization, K.K.; supervision, T.K.; project administration, T.K.; funding acquisition, K.K. All authors have read and agreed to the published version of the manuscript.

Funding: This work was funded by JSPS KAKENHI, grant number JP26K25518.

Institutional Review Board Statement: The study was conducted in accordance with the Declaration of Helsinki and approved by the Ethics Committee of Kyoto Tachibana University (protocol code 23-27 and date of approval Approved on 21 July 2023).

Informed Consent Statement: Informed consent was obtained from all subjects involved in the study. Written informed consent has been obtained from the patient(s) to publish this paper.

Data Availability Statement: The datasets generated and/or analyzed during the current study are not publicly available due to privacy and ethical restrictions but are available from the corresponding author on reasonable request.

Acknowledgments: We would like to express our gratitude to all participants involved in this research. During the preparation of this manuscript, the authors used Gemini (Google LLC, Mountain View, CA, USA) for the purposes of translation, word count reduction, and readability improvement. The authors have reviewed and edited the output and take full responsibility for the content of this publication.

Conflicts of Interest: The authors declare no conflicts of interest.

Abbreviations

The following abbreviations are used in this manuscript:

AoU	Amount of Use
DIP	Distal interphalangeal
EEG	Electroencephalography
ICA	Independent component analysis
MAL	Motor Activity Log-14
MBD	Multiple-Baseline Design
NRS	Numerical Rating Scale
PSI	Post-stroke impairment
QoM	Quality of Movement
SoA	Sense of Agency

References

1. Kanzler, C.M.; Schwarz, A.; Held, J.P.O.; Luft, A.R.; Gassert, R.; Lambercy, O. Technology-aided assessment of functionally relevant sensorimotor impairments in arm and hand of post-stroke individuals. *J. Neuroeng. Rehabil.* **2020**, *17*, 128. [CrossRef] [PubMed]
2. Lawrence, E.S.; Coshall, C.; Dundas, R.; Stewart, J.; Rudd, A.G.; Howard, R.; Wolfe, C.D.A. Estimates of the prevalence of acute stroke impairments and disability in a multiethnic population. *Stroke* **2001**, *32*, 1279–1284. [CrossRef] [PubMed]
3. Kodama, T.; Kitai, K. Clinical usefulness of real-time sensory compensation feedback training on sensorimotor dysfunction after stroke. In *Stroke—Management Pearls*; Agrawal, A., Ed.; IntechOpen: London, UK, 2023. [CrossRef]
4. Serrada, I.; Hordacre, B.; Hillier, S.L. Does sensory retraining improve sensation and sensorimotor function following stroke: A systematic review and meta-analysis. *Front. Neurosci.* **2019**, *13*, 402. [CrossRef] [PubMed]
5. Schabrun, S.M.; Hillier, S. Evidence for the retraining of sensation after stroke: A systematic review. *Clin. Rehabil.* **2009**, *23*, 27–39. [CrossRef] [PubMed]

6. Carrico, C.; Chelette, K.C., 2nd; Westgate, P.M.; Powell, E.; Nichols, L.; Fleischer, A.; Sawaki, L. Nerve stimulation enhances task-oriented training in chronic, severe motor deficit after stroke: A randomized trial. *Stroke* **2016**, *47*, 1879–1884. [CrossRef] [PubMed]
7. Minohara, R.; Wen, W.; Hamasaki, S.; Maeda, T.; Kato, M.; Yamakawa, H.; Yamashita, A.; Asama, H. Strength of Intentional Effort Enhances the Sense of Agency. *Front. Psychol.* **2016**, *7*, 1165. [CrossRef] [PubMed]
8. Sharma, N.; Cohen, L.G. Recovery of motor function after stroke. *Dev. Psychobiol.* **2012**, *54*, 254–262. [CrossRef] [PubMed]
9. Hu, X.L.; Tong, R.K.Y.; Ho, N.S.K.; Xue, J.J.; Rong, W.; Li, L.S.W. Wrist rehabilitation assisted by an electromyography-driven neuromuscular electrical stimulation robot after stroke. *Neurorehabili Neural Repair.* **2015**, *29*, 767–776. [CrossRef] [PubMed]
10. Ramachandran, V.S.; Altschuler, E.L. The use of visual feedback, in particular mirror visual feedback, in restoring brain function. *Brain* **2009**, *132*, 1693–1710. [CrossRef] [PubMed]
11. Osumi, M.; Nobusako, S.; Zama, T.; Yokotani, N.; Shimada, S.; Maeda, T.; Morioka, S. The relationship and difference between delay detection ability and judgment of sense of agency. *PLoS ONE* **2019**, *14*, e0219222. [CrossRef] [PubMed]
12. Gorniak, S.L.; Alberts, J.L. Effects of aging on force coordination in bimanual task performance. *Exp. Brain Res.* **2013**, *229*, 273–284. [CrossRef] [PubMed]
13. Kitai, K.; Odagiri, M.; Yamauchi, R.; Kodama, T. Evaluation of intervention effectiveness of sensory compensatory training with tactile discrimination feedback on sensorimotor dysfunction of the hand after stroke. *Brain Sci.* **2021**, *11*, 1314. [CrossRef] [PubMed]
14. Kitai, K.; Nishigaya, K.; Mizomoto, Y.; Ito, H.; Yamauchi, R.; Katayama, O.; Morita, K.; Murata, S.; Kodama, T. Enhancing hand sensorimotor function in individuals with cervical spinal cord injury: A novel tactile discrimination feedback approach using a multiple-baseline design. *Brain Sci.* **2025**, *15*, 352. [CrossRef] [PubMed]
15. Salis, F.; Costaggiu, D.; Mandas, A. Mini-Mental State Examination: Optimal cut-off levels for mild and severe cognitive impairment. *Geriatrics* **2023**, *8*, 12. [CrossRef] [PubMed]
16. Tombaugh, T.N. Trail Making Test A and B: Normative data stratified by age and education. *Arch. Clin. Neuropsychol.* **2004**, *19*, 203–214. [CrossRef] [PubMed]
17. Brunnstrom, S. Motor testing procedures in hemiplegia: Based on sequential recovery stages. *Phys. Ther.* **1966**, *46*, 357–375. [CrossRef] [PubMed]
18. Sullivan, M.J. The Pain Catastrophizing Scale: User Manual. Available online: https://drsandler.in/PCSmanual.pdf (accessed on 22 November 2025).
19. Fugl-Meyer, A.R.; Jääskö, L.; Leyman, I.; Olsson, S.; Steglind, S. The post-stroke hemiplegic patient. 1. a method for evaluation of physical performance. *Scand. J. Rehabil. Med.* **1975**, *7*, 13–31. [CrossRef]
20. Woodbury, M.L.; Velozo, C.A.; Richards, L.G.; Duncan, P.W. Rasch analysis staging methodology to classify upper extremity movement impairment after stroke. *Arch. Phys. Med. Rehabil.* **2013**, *94*, 1527–1533. [CrossRef] [PubMed]
21. Khojasteh, B.; Janko, M.; Visell, Y. Complexity, rate, and scale in sliding friction dynamics between a finger and textured surface. *Sci. Rep.* **2018**, *8*, 13710. [CrossRef] [PubMed]
22. Ryan, C.P.; Bettelani, G.C.; Ciotti, S.; Parise, C.; Moscatelli, A.; Bianchi, M. The interaction between motion and texture in the sense of touch. *J. Neurophysiol.* **2021**, *126*, 1375–1390. [CrossRef] [PubMed]
23. Van der Cruyssen, F.; Politis, C. Neurophysiological aspects of the trigeminal sensory system: An update. *Rev. Neurosci.* **2018**, *29*, 115–123. [CrossRef] [PubMed]
24. Horner, R.H.; Carr, E.G.; Halle, J.; McGee, G.; Odom, S.; Wolery, M. The use of single-subject research to identify evidence-based practice in special education. *Except. Child.* **2005**, *71*, 165–179. [CrossRef]
25. Andelin, L.; Reynolds, S.; Schoen, S. Effectiveness of occupational therapy using a sensory integration approach: A multiple-baseline design study. *Am. J. Occup. Ther.* **2021**, *75*, 7506205030. [CrossRef] [PubMed]
26. Kratochwill, T.R.; Hitchcock, J.; Horner, R.H.; Levin, J.R.; Odom, S.L.; Rindskopf, D.M.; Shadish, W.R. *Single-Case Designs Technical Documentation*; What Works Clearinghouse: Washington, DC, USA, 2010.
27. Julien, M.; D'Amours, J.; Leduc, M.P.; Côté, A.C.; Oziel Rodier, R.; Demers, L.; Desrosiers, J. Responsiveness of the Box and Block Test with older adults in rehabilitation. *Phys. Occup. Ther. Geriatr.* **2017**, *35*, 109–118. [CrossRef]
28. Irie, K.; Iseki, H.; Okamoto, K.; Nishimura, S.; Kagechika, K. Introduction of the Purdue Pegboard Test for fine assessment of severity of cervical myelopathy before and after surgery. *J. Phys. Ther. Sci.* **2020**, *32*, 210–214. [CrossRef] [PubMed]
29. Taub, E.; Uswatte, G.; King, D.K.; Morris, D.; Crago, J.E.; Chatterjee, A. A placebo-controlled trial of constraint-induced movement therapy for upper extremity after stroke. *Stroke* **2006**, *37*, 1045–1049. [CrossRef] [PubMed]
30. Hyvärinen, A.; Oja, E. Independent component analysis: Algorithms and applications. *Neural Netw.* **2000**, *13*, 411–430. [CrossRef] [PubMed]
31. Delorme, A.; Makeig, S. EEGLAB: An open source toolbox for analysis of single-trial EEG dynamics including independent component analysis. *J. Neurosci. Methods* **2004**, *134*, 9–21. [CrossRef] [PubMed]

32. Zhang, S.; Zhu, Z.; Zhang, B.; Feng, B.; Yu, T.; Li, Z. The CSP-based new features plus non-convex log sparse feature selection for motor imagery EEG classification. *Sensors* **2020**, *20*, 4749. [CrossRef] [PubMed]
33. Parker, R.I.; Vannest, K.J.; Davis, J.L.; Sauber, S.B. Combining nonoverlap and trend for single-case research: Tau-U. *Behav. Ther.* **2011**, *42*, 284–299. [CrossRef] [PubMed]
34. Ninci, J.; Vannest, K.J.; Willson, V.; Zhang, N. Interrater agreement between visual analysts of single-case data: A meta-analysis. *Behav. Modif.* **2015**, *39*, 510–541. [CrossRef] [PubMed]
35. Vannest, K.J.; Parker, R.I.; Gonen, O.; Adiguzel, T. *Single Case Research: Web-Based Calculators for SCR Analysis, Version 2.0*; [Web-Based Application]; Texas A&M University: College Station, TX, USA, 2016. Available online: https://singlecaseresearch.org/ (accessed on 24 March 2024).
36. Xia, M.; Wang, J.; He, Y. BrainNet Viewer: A network visualization tool for human brain connectomics. *PLoS ONE* **2013**, *8*, e68910. [CrossRef] [PubMed]
37. Winges, S.A. Somatosensory feedback refines the perception of hand shape with respect to external constraints. *Neuroscience* **2015**, *293*, 1–11. [CrossRef] [PubMed]
38. Perruchoud, D.; Murray, M.M.; Lefebvre, J.; Ionta, S. Focal dystonia and the sensory-motor integrative loop for enacting (SMILE). *Front. Hum. Neurosci.* **2014**, *8*, 458. [CrossRef] [PubMed]
39. Sakamoto, K.; Kawaguchi, N.; Mushiake, H. Shape and rule information is reflected in different local field potential frequencies and different areas of the primate lateral prefrontal cortex. *Front. Behav. Neurosci.* **2022**, *16*, 750832. [CrossRef] [PubMed]
40. Ward, N.S.; Brown, M.M.; Thompson, A.J.; Frackowiak, R.S.J. Neural correlates of outcome after stroke: A cross-sectional fMRI study. *Brain* **2003**, *126*, 1430–1448. [CrossRef] [PubMed]
41. Zemke, A.C.; Heagerty, P.J.; Lee, C.; Cramer, S.C. Motor cortex organization after stroke is related to side of stroke and level of recovery. *Stroke* **2003**, *34*, e23–e28. [CrossRef] [PubMed]
42. Wiech, K.; Ploner, M.; Tracey, I. Neurocognitive aspects of pain perception. *Trends Cogn. Sci.* **2008**, *12*, 306–313. [CrossRef] [PubMed]
43. Zagha, E.; Ge, X.; McCormick, D.A. Competing neural ensembles in motor cortex gate goal-directed motor output. *Neuron* **2015**, *88*, 565–577. [CrossRef] [PubMed]
44. Spooner, R.K.; Wiesman, A.I.; O'Neill, J.; Schantell, M.D.; Fox, H.S.; Swindells, S.; Wilson, T.W. Prefrontal gating of sensory input differentiates cognitively impaired and unimpaired aging adults with HIV. *Brain Commun.* **2020**, *2*, fcaa080. [CrossRef] [PubMed]
45. Yamashita, T.; Pala, A.; Pedrido, L.; Kremer, Y.; Welker, E.; Petersen, C.C.H. Membrane potential dynamics of neocortical projection neurons driving target-specific signals. *Neuron* **2013**, *80*, 1477–1490. [CrossRef] [PubMed]
46. van der Lee, J.H.; Wagenaar, R.C.; Lankhorst, G.J.; Vogelaar, T.W.; Devillé, W.L.; Bouter, L.M. Forced use of the upper extremity in chronic stroke patients: Results from a single-blind randomized clinical trial. *Stroke* **1999**, *30*, 2369–2375. [CrossRef] [PubMed]
47. Yanagisawa, T.; Hirata, M.; Saitoh, Y.; Kishima, H.; Matsushita, K.; Goto, T.; Fukuma, R.; Yokoi, H.; Kamitani, Y.; Yoshimine, T. Electrocorticographic control of a prosthetic arm in paralyzed patients. *Ann. Neurol.* **2012**, *71*, 353–361. [CrossRef] [PubMed]
48. Synofzik, M.; Vosgerau, G.; Newen, A. Beyond the comparator model: A multifactorial two-step account of agency. *Conscious. Cogn.* **2008**, *17*, 219–239. [CrossRef] [PubMed]
49. Miyawaki, Y.; Otani, T.; Morioka, S. Dynamic relationship between sense of agency and post-stroke sensorimotor deficits: A longitudinal case study. *Brain Sci.* **2020**, *10*, 294. [CrossRef] [PubMed]
50. Oujamaa, L.; Relave, I.; Froger, J.; Mottet, D.; Pelissier, J.Y. Rehabilitation of arm function after stroke: Literature review. *Ann. Phys. Rehabil. Med.* **2009**, *52*, 269–293. [CrossRef] [PubMed]
51. Leung, E.S.; Mofatteh, M. Investigating the feasibility and safety of osseointegration with neural interfaces for advanced prosthetic control. *Cureus* **2025**, *17*, e82567. [CrossRef] [PubMed]

Disclaimer/Publisher's Note: The statements, opinions and data contained in all publications are solely those of the individual author(s) and contributor(s) and not of MDPI and/or the editor(s). MDPI and/or the editor(s) disclaim responsibility for any injury to people or property resulting from any ideas, methods, instructions or products referred to in the content.